Accepted Manuscript

Bone Volume Fraction and Fabric Anisotropy Are Better Determinants of Trabecular Bone Stiffness than Other Morphological Variables

Dr. Ghislain Maquer[1*], MSc Sarah N. Musy[1*], Dr. Jasmin Wandel[2], Dr. Thomas Gross[3] and Prof. Philippe K. Zysset[1+]

[1] *Institute for Surgical Technology and Biomechanics, University of Bern, Stauffacherstrasse 78, 3014 Bern, Switzerland*

[2] *Institute for Risks and Extremes, Bern University of Applied Sciences, Jlcoweg 1, 3400 Burgdorf, Switzerland*

[3] *Institute of Lightweight Design and Structural Biomechanics, Vienna University of Technology, Vienna 1040, Austria*

*Ghislain Maquer and Sarah Musy contributed equally to this work and request acknowledgement of co-first authorship.

+Corresponding author: Philippe Zysset; Tel.: +41 31 631 59 25; fax: +41 31 631 59 60; E-mail address: philippe.zysset@istb.unibe.ch

Word count abstract: 282

Word count: 2761

Figures: 3

Tables: 4 + 1 supplementary table

Disclosure page

The authors hereby declare that there are no financial or personal conflicts of interest regarding this manuscript.

Abstract

As our population ages, more individuals suffer from osteoporosis. This disease leads to impaired trabecular architecture and increased fracture risk. It is essential to understand how morphological and mechanical properties of the cancellous bone are related. Morphology-elasticity relationships based on bone volume fraction (BV/TV) and fabric anisotropy explain up to 98% of the variation in elastic properties. Yet, other morphological variables such as individual trabeculae segmentation (ITS) and trabecular bone score (TBS) could improve the stiffness predictions. A total of 743 micro-computed tomography reconstructions of cubic trabecular bone samples extracted from femur, radius, vertebrae and iliac crest were analysed. Their morphology was assessed via 25 variables and their stiffness tensor ($\mathbb{C}_{\boldsymbol{FE}}$) was computed from six independent load cases using micro finite element analyses. Variance inflation factors were calculated to evaluate collinearity between morphological variables and decide upon their inclusion in morphology-elasticity relationships. The statistically admissible morphological variables were included in a multi-linear regression modelling the dependent variable $\mathbb{C}_{\boldsymbol{FE}}$. The contribution of each independent variable was evaluated (ANOVA). Our results show that BV/TV is the best determinant of $\mathbb{C}_{\boldsymbol{FE}}$ (r^2_{adj}=0.889), especially in combination with fabric (r^2_{adj}=0.968). Including the other independent predictors hardly affected the amount of variance explained by the model (r^2_{adj}=0.975). Across all anatomical sites, BV/TV explained 87% of the variance of the bone elastic properties. Fabric further described 10% of the bone stiffness, but the improvement in variance explanation by adding other independent factors was marginal (<1%). These findings confirm that BV/TV and fabric are the best determinants of trabecular bone stiffness and show, against common belief, that other morphological variables do not bring any further contribution. These overall conclusions remain to be confirmed for specific bone diseases and post-elastic properties.

Keywords: µFE, elastic properties, bone micro-structure, trabecular bone score, individual trabeculae segmentation.

Introduction

Osteoporosis is a metabolic bone disease decreasing bone strength and leading to an increased fracture risk. Beyond loss of bone mass, degradation of the trabecular microarchitecture belongs to most definitions of osteoporosis[1] and contributes to bone fragility[2]. Bone volume fraction (BV/TV), fabric anisotropy and a variety of other morphological variables accessible via micro-computed tomography (μCT), constitute potential determinants of the mechanical properties of cancellous bone.

Standard 3D parameters, inspired from stereology[3], include connectivity density, trabecular thickness, spacing, number and surface[4-12]. However, those indices have very limited value for assessing the bone elastic properties[13]. New variables were introduced by decomposing the trabecular network into rods and plates[14]. Yet, the best multi-linear models combining trabecular spacing, rod thickness and ratio rod volume over total bone volume only slightly outperformed BV/TV alone in terms of stiffness prediction[15]. Recent results from individual trabeculae segmentation (ITS) suggest that axial BV/TV and plate BV/TV may be better determinants of the elastic and yield properties of trabecular bone than BV/TV alone[16,17]. Rod-related variables were found to contribute less to bone stiffness[16,17], which contradicts prior findings[15]. The trabecular bone score (TBS) is a 2D texture parameter possibly related to trabecular structure. Initially developed on projections of μCT images, it was proposed as an ancillary use of dual energy X-ray absorptiometry (DXA) to provide complementary information for the diagnosis of osteoporosis[18,19]. However, TBS does not improve the prediction of compressive vertebral stiffness and strength provided by areal bone mineral density (aBMD) alone[20,21].

Alternatively, accounting for trabecular fabric anisotropy enhances the high correlations between bone volume fraction and stiffness[22]. In fact, with only these two variables (BV/TV and fabric), morphology-elasticity relationships can already explain more than 95% of the variation in elastic properties of trabecular bone under multi-axial tests performed

numerically (micro finite element analyses - μFEA)[23-25]. Although other morphological indices are valuable to describe the evolving trabecular architecture under disease or therapy, it is still unclear whether they can improve these stiffness predictions at all.

Relying on statistically sound multi-linear regression models of μCT and μFE data, the aim of this work is to evaluate the contribution of the eligible morphological variables in determining multi-axial elastic properties of trabecular bone.

Materials and methods

Preparation, imaging and numerical testing

μCT and μFE data from previous studies were used[26-28]. Briefly, trabecular bone sections from head, neck, greater and lesser trochanter of proximal femurs (two female donors; 66 ± 8 years), distal radius (three pairs; gender and age of the donors unknown), vertebral bodies (six male donors; 60 ± 16 years; T11, L2 and L4 levels) and iliac crests (17 male, 9 female and 16 unknown donors; 66 ± 12 years) were scanned in a μCT (μCT40, Scanco Medical , Brüttisellen, Switzerland) at a resolution of 18μm (Fig.1). After segmentation, the authors removed the unconnected bone regions and extracted 743 cubic volume elements (CVE) with a 5.3 mm side length (4 mm for the iliac crest samples) from the trabecular core[29] (264 femoral, 81 radial, 356 vertebral and 42 iliac crest samples). Then, segmented image voxels were converted into linear hexahedral elements with a Young's modulus of 12 GPa and a Poisson's ratio of 0.3[30] to generate μFE models. Three uni-axial tension and three shear tests were simulated on the CVEs with kinematic uniform boundary conditions (KUBCs)[31] and their full homogenised stiffness tensor $\mathbb{C}_{FE}$ was computed[32]. The anisotropic stiffness tensor characterizes the elastic response of trabecular bone to any possible loading.

Histomorphometry

BV/TV and the standard morphological parameters were computed via IPL (Scanco Medical, Brüttisellen, Switzerland) or ImageJ[33]. The current standards and nomenclature were used[34]. Structure model index (SMI), connectivity density (Conn.D), trabecular thickness (Tb.Th) and its standard deviation (Tb.Th.SD), spacing (Tb.Sp and Tb.Sp.SD), number (Tb.N) and surface (BS) were evaluated for the CVEs. The ITS indices were measured via the dedicated ITS analysis software of Columbia University (bit.ly/ColumbiaITS)[16,17]. This discrimination between rod and plate-like trabeculae after a topology-preserving skeletonization of the trabeculae yielded plate and rod BV/TV (pBV/TV, rBV/TV), axial BV/TV (aBV/TV), plate and rod tissue fraction (pBV/BV, rBV/BV), plate and rod trabecular number density (pTb.N, rTb.N), plate and rod trabecular thickness (pTb.Th, rTb.Th), plate trabecular surface (Tb.S), rod trabecular length (rTb.l), trabecular connection densities between plate-plate (PP Junc.D), plate-rod (PR Junc.D) and rod-rod (RR Junc.D). Trabecular bone score (TBS) was implemented in Python following the original papers[18,19]. The technique is essentially based on the experimental semi-variogram of a 2D image. Such variogram compares variations of gray-level between pairs of pixels, independently of their orientation and is widely used in geophysics for instance, assessing the roughness of a terrain[35]. The average squared difference $\gamma(h)$ of intensity values is computed between each pixel of interest P(i,j) and all its neighbouring pixels N(h), separated by a lag distance h, which is increased incrementally. The higher γ, the more variability in the image. TBS, the slope at origin of the variogram on a log-log scale, has no physical unit and reflects the variation between adjacent pixels. Two-dimensional images were created via Medtool (dr-pahr.at) by projecting the segmented µCT data of the CVEs on 3 planes x, y, z and TBS was computed for each projection[18].

Isotropic and anisotropic morphology-elasticity relationships

Among other models, the Zysset-Curnier fabric-elasticity relationship[25] was used to calculate the homogenised stiffness tensor $\mathbb{C}_{\mathrm{model}}$ of each CVE predicted by BV/TV and fabric. The anisotropy information is provided by the positive definite fabric tensor[36] determined via mean intercept length (MIL)[37]. The isotropic model is created by replacing the fabric tensor by an identity tensor[26]. A multi-linear problem was created after logarithmic transformation of the fabric-elasticity model (Figure 1). The multi-linear regression aims at minimising the sum of squared residuals between $\mathbb{C}_{model}$ and $\mathbb{C}_{FE}$, the predicted and measured homogenised stiffness tensors. To ensure the validity of such a model, both homoscedasticity (homogeneity of the variance) and normality of the residuals were checked graphically.

Predictive power of each morphological variable in isotropic and anisotropic models

To decide on the best determinant of the bone elastic properties, BV/TV was successively replaced in the Zysset-Curnier model by each morphological parameter other than fabric. While trabecular bone features an anisotropic structure adapted to external loadings, accounting for trabecular fabric anisotropy enhances significantly the stiffness predictions of BVTV-based isotropic models[22]. Fabric was therefore chosen as the 2nd independent predictor. Anisotropic and isotropic models were then tested by accounting for or neglecting the fabric in the calculations. Their adjusted coefficients of determination (r^2_{adj}) between measured ($\mathbb{C}_{FE}$) and predicted ($\mathbb{C}_{model}$) stiffness tensors and their residual standard errors (RSE) were computed.

Selection of the independent parameters

A multi-linear model is mathematically valid if it includes only independent factors. High correlations among explanatory variables are likely to cause multicollinearity, which artificially inflates the variance of the estimated regression coefficients compared to a model

with independent variables and consequently, the estimators cannot be trusted for prediction. Since high correlations were previously found between several variables, a selection based on the variance inflation factor (VIF) was performed in R 3.0.1 (r-project.org) using the package *vif*[38] to detect independent variables and avoid multicollinearity and overfitting of the model. VIF quantifies the variance-inflation of a regression coefficient due to multicollinearity. Parameters with the highest VIF values, except BV/TV that is the best determinant, were successively rejected from a multi-linear regression system that originally included all available morphological parameters and the VIF of the remaining factors were re-computed after each elimination. Eventually, parameters whose VIF value was lower than 4 were considered independent[39] and introduced in a new multi-linear regression: the global model.

Comparison of isotropic, anisotropic and global models

Adjusted coefficient of determination against $\mathbb{C}_{\boldsymbol{FE}}$ (r^2_{adj}), residual standard error (RSE) and their 95% confidence interval back-transformed into the normal scale (CI)[40] of the three statistically admissible multi-linear models (isotropic, anisotropic and global) were compared to determine the improvement following inclusion of fabric and other independent parameters.

Potentially, each new variable added to a model further explains the variation in bone elastic properties. The extra contribution provided by each variable to the global model was evaluated using ANOVA (analysis of variance) and defined as the percentage of variation "additionally" explained by the newly introduced variable.

Results

Our models were validated by checking homoscedasticity of the morphological variables and normality of the residuals. In addition to a pooled dataset ("Combined"), the analyses were also conducted for each individual location because of various degrees of anisotropy (Table

1) and small but significant differences in the predicted stiffness tensor (Table 4) found between different anatomical locations.

No surprises arose from the replacement of BV/TV by other variables in the isotropic and anisotropic morphology-elasticity models. Even though pBV/TV provided slightly better results for the vertebral samples, the study confirmed that BV/TV is the best determinant for the elastic properties of bone in general ($0.730 < r^2_{adj} < 0.983$). Accounting for fabric anisotropy improves the predictions of all variables, independently of the location (Table 2).

Correlations between the morphological parameters (Table A1) confirmed that, unlike DA ($r^2 < 0.148$), BV/TV is highly correlated with most variables ($0.341 < r^2 < 0.99$). BV/TV being the best stiffness predictor, evaluation of its collinearity with the other morphological parameters, was necessary before their inclusion in a multi-linear model. Besides BV/TV and fabric, the stepwise VIF selection (Table 3) yielded independent parameters for each anatomical site (SMI, Tb.Th.SD, Tb.Sp.SD, pTb.Th, rTb.Th, p.Tb.S, r.Tb.l, RR.Junc.D, TBS). They were added to the anisotropic model to form location-specific global models.

The predictive powers of the three models were then compared. Adding fabric anisotropy to an isotropic model based on BV/TV greatly improved its stiffness predictions. Adding other independent parameters to an anisotropic model had marginal effects. From the isotropic to the anisotropic model the amelioration was 13% for r^2_{adj} and 50% for RSE, but only 0.7% for r^2_{adj} and 12% for RSE from the anisotropic to the global model (Table 4). Therefore, the width of the confidence intervals of the residuals reduced drastically with the introduction of fabric, but the global model did not change the width relevantly (Figure 2).

The contribution of each additional independent variable included in the global model was evaluated for all anatomical locations. In the radius, the most anisotropic location, the contribution of BV/TV was the lowest (73%) and the percentage of variation explained by fabric the highest (24%). Yet, generally, BV/TV was the parameter contributing the most to the variance explanation of the bone elastic properties (~87%), fabric described around 10%

more, but the improvement in variance explanation by adding other independent factors was marginal (<1%), even compared to the residuals' (~3%).

Discussion

A strong relation between fabric and stiffness tensors has been demonstrated since the early 80's[36] and confirmed ever since. Bone features an optimized structure[41] and relationships based on BV/TV and fabric remain valid across anatomical locations[22,26] and bone diseases such as osteoporosis[24] or hypoparathyroidism[27]. Continuum FE models already rely on the material constants determined from the homogenisation of trabecular cubes. They predict stiffness and strength of bone as well as μFE[42], hence better than morphological parameters[43]. Finally, research now focuses on deriving fabric tensors from conventional CTs, either via gradient-based methods or mapping of μCT information[44-47]. Nevertheless, morphological variables are still combined into multi-linear models to predict the mechanical properties of cancellous bone[14-17,21,45], but never compared to a combination BV/TV-fabric. In this study, a systematic analysis of the stiffness and morphology of 743 samples extracted from femur, radius, iliac crest and vertebral body was performed to determine the relevant predictors of the bone elastic properties. It is now clear that, together, bone volume fraction and fabric anisotropy are the best explanatory variables to the elastic behaviour of trabecular bone, in general. After verification, this might even get extended to its post-elastic behaviour since stiffness, yield and ultimate strength of spongious bone are highly correlated[48-50].

A major strength of the study is that it is not limited to the standard morphological indices, but also includes variables from non-conventional techniques such as TBS and ITS in the analysis. Aside from these two variables, few morphological factors such as TBS, Tb.Sp.SD or rTb.Th were not collinearly related with each other. Since its conception, TBS is presented as a parameter reflecting bone microarchitecture from DXA images[19] and the method receives much enthusiasm[51-54]. Yet, the point is: TBS does not correlate with any microarchitectural parameter in our study. Previously, contradictory correlations have even

been reported across anatomical sites and studies[20]. Other standard and ITS parameters have been reported by Liu et al.[16], but the authors did not account for the anisotropy of the trabecular structure. They also constituted different regression models for each individual elastic and shear modulus, although a single orthotropic stiffness tensor represents the elastic behaviour of bone for six canonical load cases accurately[26]. The selection of the morphological variables also differed from our study. Liu et al. successively added eligible independent factors with the highest statistical strength to their multi-linear model. By quantifying the artificial inflation of variance due to multicollinearity, the stepwise selection based on the variance inflation factor (VIF) performed in our study prevents overfitting of the model[39] and constitutes yet another strength of our work.

The isotropic regression solely based on BV/TV can already explain between 73% and 91.7% of the variation in elastic properties of iliac crest and radius, the most isotropic and anisotropic sites. Accounting for fabric raised the adjusted coefficient of determination r^2_{adj} to a minimum of 95.5%. Other morphological parameters potentially contained information to describe the remaining 4.5%. However, accounting for the independent TBS, standard and ITS indices in the anisotropic model improved the r^2_{adj} by only 0.02% maximum and hardly affected the estimates (Figure 2). Those results raise concerns. First, TBS is not related to the elastic properties of trabecular bone. Our implementation is based on the original description[18,19] and the lack of relation of TBS with stiffness and strength has already been reported[20,21]. From a mechanical standpoint, it remains therefore unclear how TBS can contribute to predict vertebral fracture risk. Due to the stepwise VIF selection, the ITS variables included in the global model were the least related to BV/TV and their input in terms of stiffness predictions was negligible. However, pBV/TV, bone volume fraction of the plate-like trabeculae, and aBV/TV, bone volume fraction of the trabeculae oriented in the axial directions, are potentially good substitutes for BV/TV[17]. Simply, BV/TV does not require extra discrimination between rod and plates and the orientation of the trabecular

structures is already included in the fabric tensor. Moreover, for known bone tissue mineralization, BV/TV can be directly estimated from BMD[55].

FE analysis has a number of key advantages with respect to direct mechanical testing: high reproducibility, no sample preparation artefacts, no damage-related boundary artefacts and no restriction in the number of assessed elastic constants. Any morphological feature that is captured in the µCT reconstruction at 18 µm is reflected in the FE analysis. Accordingly, we believe that FE analysis is the best-suited method to investigate the influence of morphology on the elasticity of trabecular bone. The limitation of our FE analysis is the assumption of homogenous and isotropic tissue material properties. A Young's modulus of 12 GPa has been chosen according to our experimental results from nano-indentation. In the used linear FE analysis, the apparent stiffnesses scale linearly with tissue modulus and the latter does therefore not affect the morphology-elasticity relationships. On the other hand, a previous study demonstrated that the heterogeneous tissue mineralization has only a minor influence on apparent trabecular bone elasticity[56]. Finally, anisotropy of the bone extracellular matrix is not expected to influence substantially our results as the structural elements are mostly loaded along their principal axis. A common limitation regarding the mechanical testing of bone is the type of boundary conditions. Generally, kinematic uniform boundary conditions (KUBCs) are chosen, but KUBCs overestimate the apparent stiffness of the CVEs and rather mimics trabecular bone adjacent to a rigid neighbourhood, such as cortical bone. Periodicity-compatible mixed uniform boundary conditions (PMUBCs) are more appropriate to evaluate samples extracted from the cancellous core[30]. The BV/TV and fabric-based Zysset-Curnier model copes with both boundary conditions equally well[56], but KUBCs are generally performed in the literature.

Morphological parameters are very valuable for characterization of the trabecular microstructure and its evolution during modelling and remodelling processes. Yet, bone volume fraction and fabric anisotropy are, together, better determinants of the trabecular bone

stiffness than the TBS, standard and ITS morphological indices. To provide better assessment of trabecular mechanics *in vivo*, research should focus on the imaging devices and methods in order to improve the precision of BV/TV and to include bone anisotropy, something already possible at the extremities via high-resolution peripheral quantitative CT.

Acknowledgements

The authors thank Prof. Edward Guo and Ji Wang (Bone Bioengineering Laboratory, Columbia University, U.S.) for their assistance with the ITS analysis software and Dr. Dieter Pahr (Institute for Lightweight Design and Structural Biomechanics, Vienna University of Technology, Austria) for his support with Medtool. The authors acknowledge Prof. Ralph Müller (Institute for Biomechanics, ETH Zurich, Switzerland) for providing µCT data of iliac crests and Jarunan Panyasantisuk (Institute for Surgical Technology and Biomechanics, University of Bern, Switzerland) for helping with the interpretation of the µFE data.

Study design: PZ; Study conduct: SM, GM, PZ; Data collection: TG; Data analysis: SM, JW; Data interpretation: GM, PZ, SM; Drafting manuscript: GM, SM; Revising manuscript content: GM, SM, PZ, JW, TG; Approving final version of manuscript: GM, SM, JW, TG, PZ; PZ and GM take responsibility for the integrity of the data analysis.

References

1. Consensus Development Conference. Osteoporosis prevention, diagnosis, and therapy. NIH Consens Statement. 2000;17:1–45.
2. Dempster DW. The contribution of trabecular architecture to cancellous bone quality. J. Bone Miner. Res. 2000;15:20–23.
3. Weibel ER. Stereological methods. Academic Press, London. 1980;2:253-257.
4. Hildebrand T, Laib A, Müller R, Dequeker J, Rüegsegger P. Direct three-dimensional morphometric analysis of human cancellous bone: microstructural data from spine, femur, iliac crest, and calcaneus. J. Bone Miner. Res. 1999;14(7):1167-1174.
5. Hildebrand T, Rüegsegger P. Quantification of Bone Microarchitecture with the Structure Model Index. CMBBE. 1997;1(1):15-23.
6. Odgaard A, Gundersen HJ. Quantification of connectivity in cancellous bone, with special emphasis on 3-D reconstructions. Bone. 1993;14(2):173-182.
7. Kabel J, Odgaard A, Van Rietberben B, Huiskes R. Connectivity and the elastic properties of cancellous bone. Bone. 1999;24(2):115-120.
8. Hildebrand T, Rüegsegger P. A new method for the model-independent assessment of thickness in three-dimensional images. J. Microsc. 1997;185(1):67-75.

9. Parfitt AM, Drezner MK, Glorieux FH, Kanis JA, Malluche H, Meunier PJ, et al. Bone histomorphometry: standardization of nomenclature, symbols, and units: report of the ASBMR histomorphometry nomenclature committee. J. Bone Miner. Res. 1987;2(6):595-610.
10. Müller R, Hildebrand T, Rüegsegger P. Non-invasive bone biopsy: a new method to analyse and display the three-dimensional structure of trabecular bone. Phys. Med. Biol. 1994;39(1):145-164.
11. Odgaard A. Three-dimensional methods for quantification of cancellous bone architecture. Bone. 1997;20(4):315-328.
12. Dempster DW, Compston JE, Drezner MK, Glorieux FH, Kanis JA, Malluche H, et al. Standardized nomenclature, symbols, and units for bone histomorphometry: A 2012 update of the Report of the ASBMR Histomorphometry Nomenclature Committee. J. Bone Miner. Res. 2013;28:1–16
13. Uchiyama T, Tanizawa T, Muramatsu H, Endo N, Takahashi HE, Hara T. Three-dimensional microstructural analysis of human trabecular bone in relation to its mechanical properties. Bone. 1999;25(4):487-491.
14. Stauber M, Müller R. Volumetric spatial decomposition of trabecular bone into rods and plates—a new method for local bone morphometry. Bone. 2006;38(4):475-484.
15. Stauber M, Rapillard L, van Lenthe GH, Zysset P, Müller R. Importance of individual rods and plates in the assessment of bone quality and their contribution to bone stiffness. J. Bone Miner. Res. 2006;21(4):586-595.
16. Liu XS, Sajda P, Saha PK, Wehrli FW, Bevill G, Keaveny TM, et al. Complete volumetric decomposition of individual trabecular plates and rods and its morphological correlations with anisotropic elastic moduli in human trabecular bone. J. Bone Miner. Res. 2008;23(2):223-235.
17. Zhou B, Liu XS, Wang J, Lu XL, Fields AJ, Guo XE. Dependence of mechanical properties of trabecular bone on plate-rod microstructure determined by individual trabecula segmentation (ITS). J. Biomech. 2014;47(3):702-708.
18. Pothuaud L, Carceller P, Hans D. Correlations between grey-level variations in 2D projection images (TBS) and 3D microarchitecture: applications in the study of human trabecular bone microarchitecture. Bone. 2008;42(4):775-787.
19. Pothuaud L, Barthe N, Krieg MA, Mehsen N, Carceller P, Hans D. Evaluation of the potential use of trabecular bone score to complement bone mineral in the diagnosis of osteoporosis: a preliminary spine BMD-matched, case-control study. J. Clin. Densitom. 2009;12(2):170-176.
20. Bousson V, Bergot C, Sutter B, Levitz B, Cortet B. Trabecular bone score (TBS): available knowledge, clinical relevance, and future prospect. Osteoporis Int. 2012;23(5):1489-1501.
21. Roux JP, Wegrzyn J, Boutroy S, Bouxsein ML, Hans D, Chapurlat R. The predictive value of trabecular bone score (TBS) on whole lumbar vertebrae mechanics: an ex vivo study. Osteoporis Int. 2013;24(9):2455-2460.
22. Matsuura M, Eckstein F Lochmüller EM, Zysset PK. The role of fabric in the quasi-static compressive mechanical properties of human trabecular bone from various anatomical locations. Biomech. Model. Mechan. 2008;7(1): 27-42.
23. Van Rietbergen B, Odgaard A, Kabel J, Huiskes R. Relationships between bone morphology and bone elastic properties can be accurately quantified using high-resolution computer reconstructions. J. Orthop. Res. 1998;16(1):23-28.
24. Homminga J, Mccreadie BR, Weinans H, Huiskes R. The dependence of the elastic properties of osteoporotic cancellous bone on volume fraction and fabric. J. Biomech. 2003;36(10):1461-1467.
25. Zysset PK. A review of morphology-elasticity relationships in human trabecular bone: theories and experiments. J. Biomech. 2003;36(10):1469-1485.

26. Gross T, Pahr DH, Zysset PK. Morphology-elasticity relationships using decreasing fabric information of human trabecular bone from three major anatomical locations. Biomech. Model. Mechan. 2013;12(4):793-800.
27. Gross T, Pahr DH, Müller R, Rubin MR, Bilezikian JP, Zysset PK. Morphology-elasticity relationships in iliac crest biopsies are not affected by hypoparathyroidism. Proc. 18th Congress of the European Society of Biomechanics (ESB), Lisbon, Portugal, July 1-4, J. Biomech. 2012;45:S253.
28. Rubin MR, Dempster DW, Kohler T, Stauber M, Zhou H, Shane E, et al. Three dimensional cancellous bone structure in hypoparathyroidism. Bone. 2010;46(1):190-195.
29. Harrigan TP, Jasty M, Mann RW, Harris WH. Limitations of the continuum assumption in cancellous bone. J. Biomech. 1988;21(4):269-275.
30. Wolfram U, Wilke HJ, Zysset PK. Valid micro finite element models of vertebral trabecular bone can be obtained using tissue properties measured with nanoindentation under wet conditions. J. Biomech. 2010;43(9):1731-1737.
31. Pahr DH, Zysset PK. Influence of boundary conditions on computed apparent elastic properties of cancellous bone. Biomech. Model. Mechan. 2008;7(6):463-476.
32. Van Rietbergen B, Odgaard A, Kabel J, Huiskes R. Direct mechanics assessment of elastic symmetries and properties of trabecular bone architecture. J. Biomech. 1996;29(12):1653-1657.
33. Doube M, Klosowski MM, Arganda-Carreras I, Cordelières FP, Dougherty RP, Jackson JS, et al. Bonej: free and extensible bone image analysis in Imagej. Bone. 2010;47(6):1076-1079.
34. Bouxsein ML, Boyd SK, Christiansen BA, Guldberg RE, Jepsen KJ, Müller R. Guidelines for assessment of bone microstructure in rodents using micro–computed tomography. J. Bone Miner. Res. 2010;25: 1468–1486.
35. Smith MW. Roughness in the Earth Sciences. Earth-Sci. Rev. 2014;136:202-225.
36. Cowin SC. The relationship between the elasticity and the fabric tensor. Mech. Mater. 1985;4(2):137-147.
37. Odgaard A, Kabel J, van Rietbergen B, Dalstra M, Huiskes R. Fabric and elastic principal directions of cancellous bone are closely related. J. Biomech. 1997;30(5):487-495.
38. Lin D, Foster DP, Ungar LH. VIF regression: A fast regression algorithm for large data. J. Am. Stat. Assoc. 2011;106(493):232-247.
39. Peat J., Barton B. Continuous Data Analyses: Correlation and Regression, in Medical Statistics: A Guide to Data Analysis and Critical Appraisal, Blackwell Publishing Inc., Malden, Massachusetts, USA. 2005. doi: 10.1002/9780470755945.ch6
40. Jørgensen E, Pedersen AR. How to obtain those nasty standard errors from transformed data and why they should not be used. (Aarhus Univ, Det Jordbrugsvidenskabelige Fakultet, Aarhus, Denmark), International Report 7. (URL: http://gbi.agrsci.dk/~ejo/publications/dinapig/intrep7.pdf)
41. Wolff J. Das gesetz der transformation der knochen. Deut. Med. Wochenschr. 1892;19:1222-1224.
42. Pahr DH, Dall'Ara E, Varga P, Zysset PK. HR-pQCT-based homogenised finite element models provide quantitative predictions of experimental vertebral body stiffness and strength with the same accuracy as μFE models. CMBBE. 2012;15(7):711-720.
43. Boutroy S, Van Rietbergen B, Sornay-Rendu E, Munoz F, Bouxsein ML, Delmas PD. Finite element analysis based on in vivo HR-pQCT images of the distal radius is associated with wrist fracture in postmenopausal women. J. Bone Miner. Res. 2008;23(3):392-399.

44. Larsson D, Luisier B, Kersh ME, Dall'Ara E, Zysset PK. Pandy MGm et al. Assessment of Transverse Isotropy in Clinical-Level CT Images of Trabecular Bone Using the Gradient Structure Tensor. Ann. Biomed. Eng. 2014;42(5):950-959.
45. Kazembakhshi S, Luo Y Constructing anisotropic finite element model of bone from computed tomography (CT). Bio-Med. Mater. Eng. 2014;24(6):2619-2626.
46. Enns-Bray WS, Owoc JS, Nishiyama KK, Boyd SK. Mapping anisotropy of the proximal femur for enhanced image based finite element analysis. J. Biomech. 2014;47(13):3272–3278.
47. Marangalou JH, Ito K, van Rietbergen B. A novel approach to estimate trabecular bone anisotropy from stress tensors. Biomech. Model. Mechan. 2014:1-10.
48. Goulet RW, Goldstein SA, Ciarelli MJ, Kuhn JL, Brown MB, Feldkamp LA. The relationship between the structural and orthogonal compressive properties of trabecular bone. J. Biomech. 1994;27(4):375-389.
49. Keaveny TM, Wachtel, EF, Ford CM, Hayes WC. Differences between the tensile and compressive strengths of bovine tibial trabecular bone depend on modulus. J. Biomech. 1994;27(9):1137-1146.
50. Hou FJ, Lang SM, Hoshaw SJ, Reimann DA, Fyhrie DP. Human vertebral body apparent and hard tissue stiffness. J. Biomech. 1998;31(11):1009-1015.
51. Pedrazzoni M, Casola, A., Verzicco I, Abbate B, Vescovini R, Sansoni P. Longitudinal changes of trabecular bone score after estrogen deprivation: effect of menopause and aromatase inhibition. J. Endocrinol. Invest. 2014;37(9):871-874.
52. Krueger D, Fidler E, Libber J, Aubry-Rozier B, Hans D, et al. Spine trabecular bone score subsequent to bone mineral density improves fracture discrimination in women. J. Clin. Densitom. 2014;17(1):60-65.
53. Nassar K, Paternotte S, Kolta S, Fechtenbaum J, Roux C, Briot, K. Added value of trabecular bone score over bone mineral density for identification of vertebral fractures in patients with areal bone mineral density in the non-osteoporotic range. Osteoporis Int. 2014;25(1):243-249.
54. Leslie WD, Aubry-Rozier B, Lix LM, Morin SN, Majumdar SR, et al. Spine bone texture assessed by trabecular bone score (TBS) predicts osteoporotic fractures in men: The Manitoba Bone Density Program. Bone. 2014;67:10-14.
55. Gross T, Pahr DH, Peyrin F, Zysset PK. Mineral heterogeneity has a minor influence on the apparent elastic properties of human cancellous bone: a SRμCT-based finite element study. CMBBE. 2012;15(11):1137-1144.
56. Panyasantisuk J, Pahr DH, Gross T, Zysset PK. Comparison of Mixed and Kinematic Uniform Boundary Conditions in Homogenized Elasticity of Femoral Trabecular Bone using Micro Finite Element Analyses. J Biomech Eng. 2014;doi: 10.1115/1.4028968

Figure

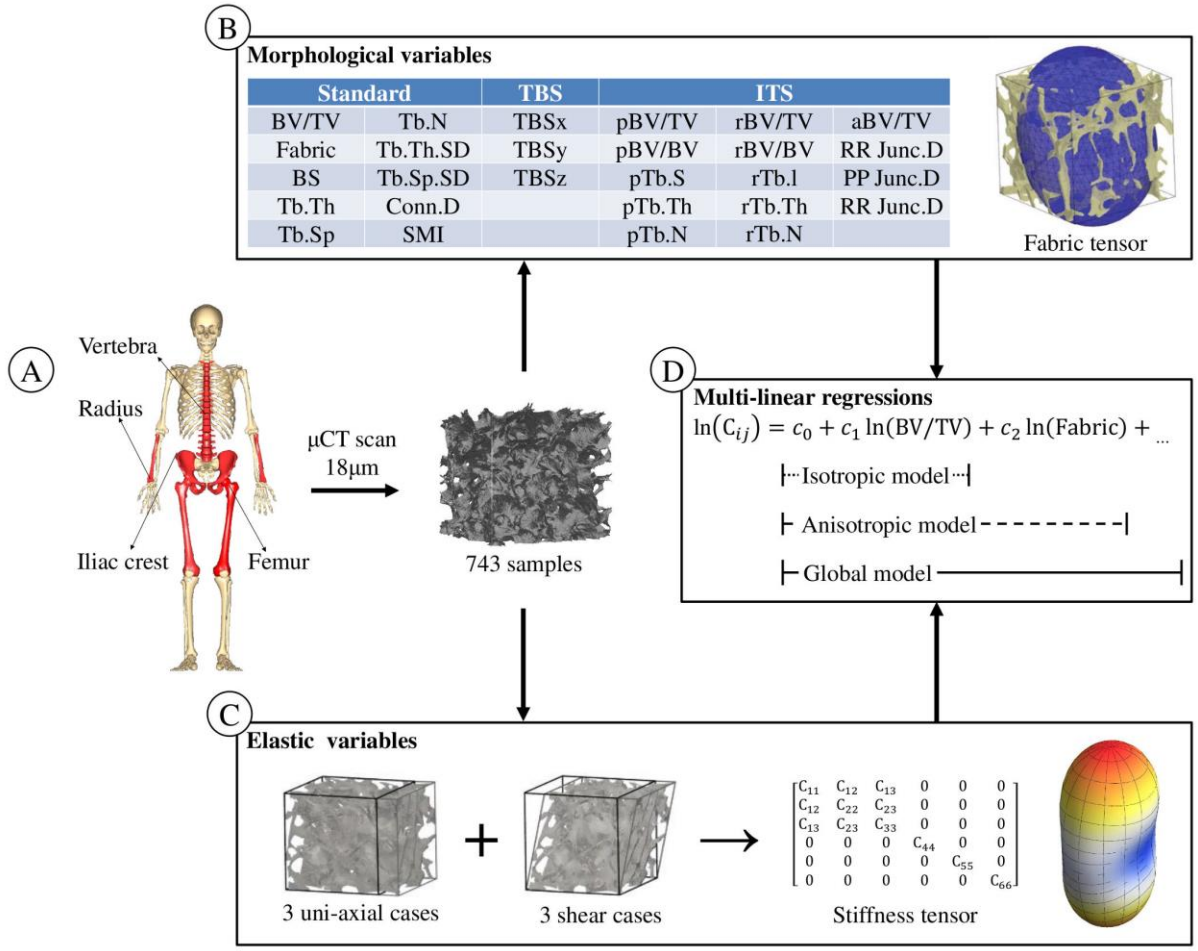

Figure 1. Bone sections were selected from various anatomical sites and scanned in µCT and cubic samples were extracted from each image (A). Independent standard, TBS and ITS variables computed for each cube (B), were used in morphology-elasticity relationships to predict its stiffness tensor calculated from µFEA (C). The predictive power of three classes of relationships was evaluated: isotropic (single variable), anisotropic (with fabric tensor) and global model including also all the other independent variables (D).

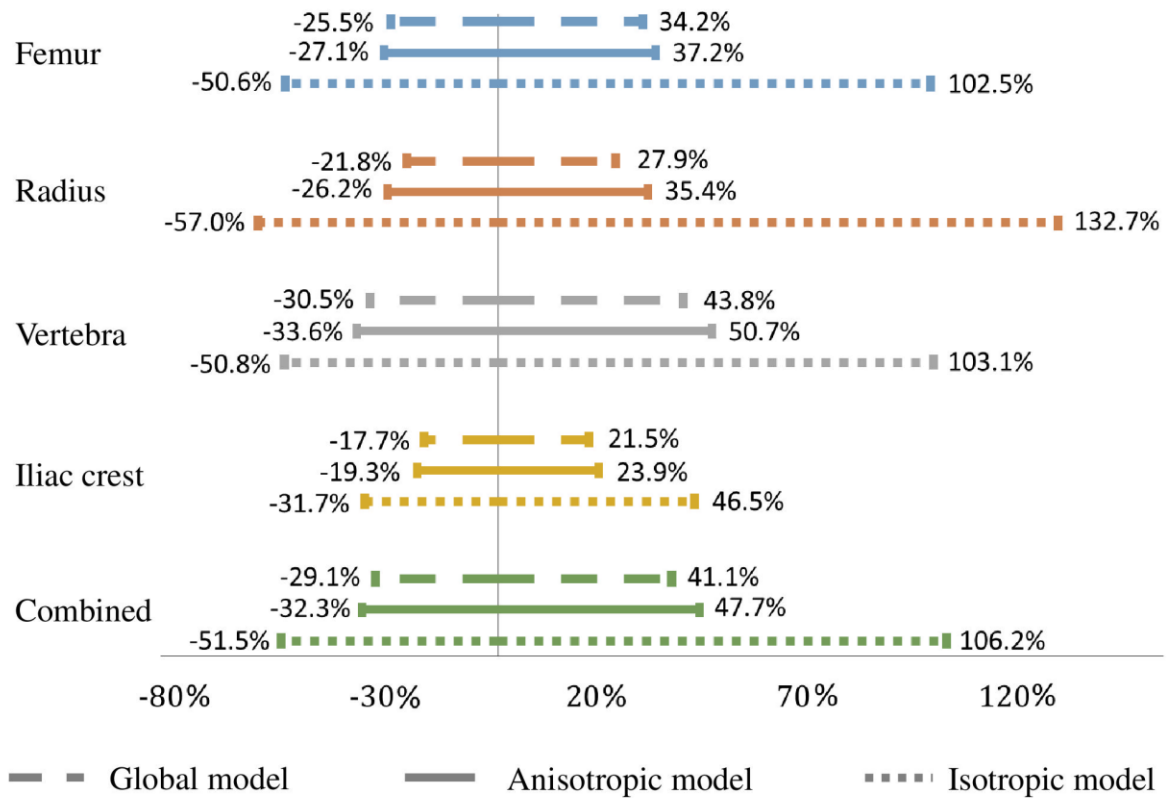

Figure 2. Confidence intervals of the relative errors in estimating the elastic properties in the direct scale after back-transformation from the log scale. The confidence intervals reduced drastically with the introduction of fabric, but the global model, which also included other independent morphological variables (SMI, Tb.Th.SD, Tb.Sp.SD, pTb.Th, rTb.Th, p.Tb.S, r.Tb.l, RR.Junc.D and TBS), did not change the width relevantly.

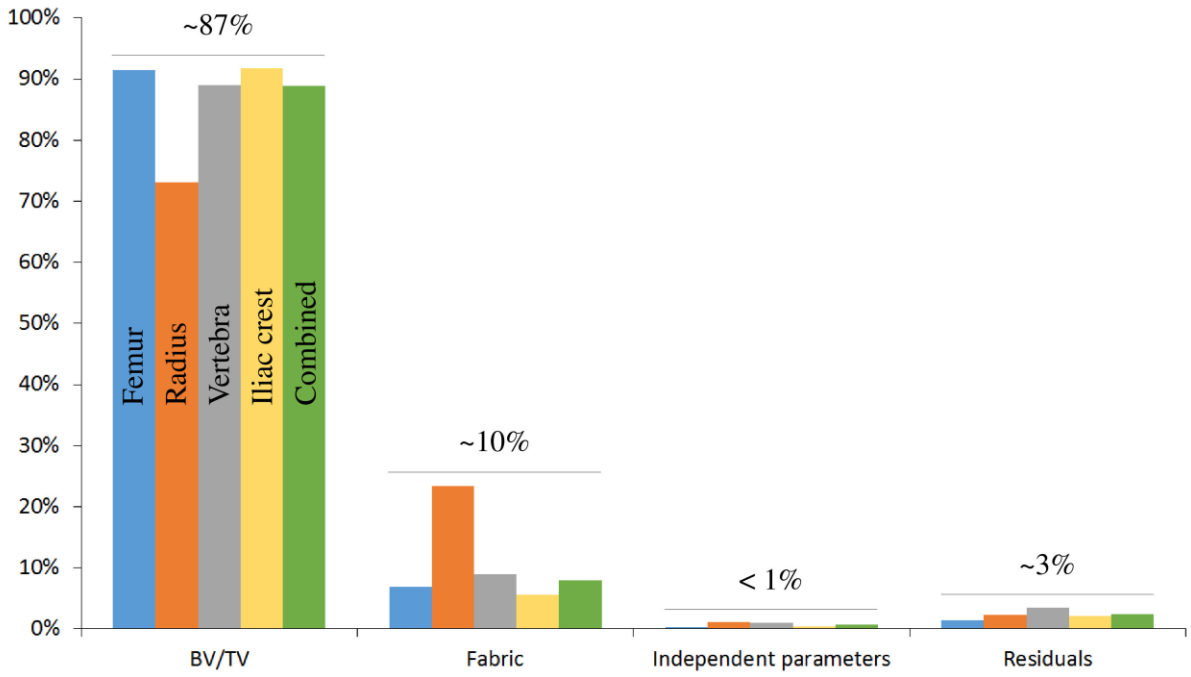

Figure 3. The relative contribution of each variable. Bone volume fraction (BV/TV) and fabric anisotropy explained most of the elastic properties of bone. The contribution of the other parameters found independent (SMI, Tb.Th.SD, Tb.Sp.SD, pTb.Th, rTb.Th, p.Tb.S, r.Tb.l, RR.Junc.D and TBS) was less than the residuals.

Tables

Table 1. Mean and standard deviation of bone volume fraction (BV/TV) and degree of anisotropy (DA) for each anatomical location and the pooled data.

	BV/TV	**DA**
Femur	0.187 ± 0.114	1.738 ± 0.241
Radius	0.165 ± 0.039	1.870 ± 0.339
Vertebra	0.113 ± 0.040	1.519 ± 0.214
Iliac crest	0.170 ± 0.068	1.453 ± 0.177
Combined	0.136 ± 0.074	1.627 ± 0.297

Table 2. Adjusted coefficient of determination (r^2_{adj}) against the measured stiffness tensor and standard error of estimate (SEE [MPa]) determined the best model, highlighted in grey.

			Isotropic					**Anisotropic**				
			Femur	*Radius*	*Vertebra*	*Iliac crest*	*Combined*	*Femur*	*Radius*	*Vertebra*	*Iliac crest*	*Combined*
Standard	**BV/TV**	r^2_{adj}	0.914	0.730	0.867	0.917	0.889	0.983	0.965	0.955	0.974	0.968
		SEE	0.360	0.432	0.362	0.196	0.369	0.161	0.155	0.209	0.110	0.199
	Conn.D	r^2_{adj}	0.465	0.581	0.651	0.644	0.395	0.529	0.812	0.745	0.700	0.469
		SEE	0.899	0.538	0.585	0.405	0.864	0.843	0.360	0.500	0.372	0.809
	SMI	r^2_{adj}	0.764	0.672	0.713	0.850	0.336	0.834	0.912	0.815	0.909	0.416
		SEE	0.597	0.476	0.531	0.263	0.905	0.501	0.247	0.426	0.205	0.849
	Tb.N	r^2_{adj}	0.734	0.625	0.739		0.607	0.798	0.867	0.828		0.682
		SEE	0.634	0.509	0.506		0.701	0.552	0.303	0.411		0.630
	Tb.Th	r^2_{adj}	0.792	0.523	0.371	0.750	0.507	0.859	0.763	0.481	0.807	0.594
		SEE	0.560	0.574	0.785	0.340	0.780	0.462	0.405	0.714	0.299	0.708
	Tb.Sp	r^2_{adj}	0.696	0.549	0.670	0.729	0.640	0.763	0.796	0.761	0.785	0.717
		SEE	0.678	0.558	0.569	0.354	0.667	0.599	0.376	0.484	0.315	0.591
	BS	r^2_{adj}	0.835	0.681	0.816	0.824	0.592	0.905	0.921	0.905	0.882	0.671
		SEE	0.499	0.470	0.425	0.285	0.709	0.378	0.234	0.306	0.233	0.637
	Tb.Th.SD	r^2_{adj}	0.567	0.543	0.433	0.699	0.327	0.641	0.781	0.539	0.757	0.412
		SEE	0.808	0.562	0.746	0.372	0.911	0.736	0.389	0.672	0.335	0.852
	Tb.Sp.SD	r^2_{adj}	0.403	0.493	0.483	0.655	0.444	0.475	0.740	0.584	0.711	0.526
		SEE	0.950	0.592	0.712	0.399	0.828	0.891	0.424	0.638	0.365	0.765
ITS	**pBV/TV**	r^2_{adj}	0.908	0.714	0.871	0.914	0.889	0.979	0.955	0.962	0.973	0.968
		SEE	0.374	0.445	0.355	0.199	0.369	0.178	0.176	0.193	0.112	0.199
	rBV/TV	r^2_{adj}	0.314	0.494	0.412	0.638	0.886	0.376	0.734	0.515	0.695	0.966
		SEE	1.018	0.591	0.759	0.409	0.375	0.971	0.429	0.690	0.375	0.205
	aBV/TV	r^2_{adj}	0.831	0.637	0.824	0.868	0.372	0.896	0.887	0.912	0.925	0.449
		SEE	0.506	0.501	0.416	0.247	0.881	0.397	0.280	0.293	0.186	0.824
	pBV/BV	r^2_{adj}	0.673	0.560	0.664	0.714	0.782	0.755	0.813	0.770	0.775	0.861
		SEE	0.703	0.551	0.574	0.363	0.518	0.609	0.360	0.475	0.322	0.413
	rBV/BV	r^2_{adj}	0.683	0.559	0.643	0.704	0.592	0.769	0.812	0.750	0.766	0.678
		SEE	0.692	0.552	0.591	0.369	0.709	0.591	0.360	0.495	0.329	0.631
	pTb.N	r^2_{adj}	0.855	0.713	0.813	0.748	0.611	0.919	0.942	0.902	0.803	0.699
		SEE	0.468	0.445	0.428	0.341	0.692	0.351	0.200	0.310	0.301	0.609
	rTb.N	r^2_{adj}	0.408	0.526	0.532	0.637	0.688	0.468	0.760	0.628	0.694	0.759
		SEE	0.946	0.572	0.677	0.409	0.620	0.897	0.407	0.604	0.376	0.545
	pTb.Th	r^2_{adj}	0.704	0.486	0.371	0.733	0.340	0.773	0.730	0.480	0.790	0.416
		SEE	0.669	0.596	0.785	0.351	0.903	0.586	0.432	0.714	0.311	0.849
	rTb.Th	r^2_{adj}	0.272	0.536	0.414	0.636	0.449	0.345	0.774	0.523	0.694	0.537
		SEE	1.049	0.566	0.758	0.410	0.824	0.995	0.396	0.684	0.376	0.756
	pTb.S	r^2_{adj}	0.309	0.484	0.367	0.667	0.281	0.395	0.729	0.477	0.728	0.366
		SEE	1.022	0.597	0.788	0.392	0.942	0.956	0.433	0.716	0.354	0.885
	rTb.l	$^2_{adj}$	0.634	0.544	0.755	0.640	0.358	0.706	0.782	0.849	0.698	0.450
		SEE	0.743	0.562	0.490	0.408	0.890	0.666	0.388	0.384	0.373	0.824
	RRJunc.D	r^2_{adj}	0.221	0.484	0.390	0.643	0.338	0.298	0.728	0.495	0.702	0.416
		SEE	1.085	0.597	0.774	0.406	0.904	1.030	0.433	0.703	0.371	0.849
	RPJunc.D	r^2_{adj}	0.740	0.587	0.718	0.667	0.285	0.798	0.816	0.809	0.722	0.371
		SEE	0.627	0.534	0.525	0.392	0.939	0.553	0.357	0.433	0.358	0.881
	PPJunc.D	r^2_{adj}	0.838	0.641	0.774	0.733	0.498	0.900	0.869	0.864	0.788	0.569
		SEE	0.495	0.498	0.471	0.351	0.787	0.389	0.301	0.366	0.313	0.729
TBS	**TBS_x**	r^2_{adj}	0.253	0.497	0.371	0.659	0.271	0.329	0.737	0.480	0.716	0.354
		SEE	1.063	0.590	0.786	0.397	0.948	1.007	0.426	0.714	0.362	0.893
	TBS_y	r^2_{adj}	0.520	0.487	0.366	0.683	0.345	0.585	0.731	0.476	0.741	0.428
		SEE	0.852	0.595	0.788	0.382	0.899	0.791	0.431	0.717	0.346	0.840
	TBS_z	$^2_{adj}$	0.297	0.502	0.377	0.641	0.363	0.368	0.748	0.484	0.699	0.447
		SEE	1.031	0.587	0.781	0.407	0.887	0.977	0.417	0.711	0.373	0.826

Table 3. Variance Inflation Factors (VIF) of the morphological indices at the first and final steps of the VIF selection. Variables with a VIF lower than 4 were considered independent and used in the global model.

		Femur		*Radius*		*Vertebra*		*Iliac crest*		*Combined*	
		First	Final	First	Final	First	Final	First	Final	First	Final
Standard	**BV/TV**	$5.7 \cdot 10^{6}$	3.3	$2.7 \cdot 10^{4}$	3.7	$2.2 \cdot 10^{4}$	2.3	$4.7 \cdot 10^{6}$	2.3	$6.2 \cdot 10^{4}$	3.4
	Fabric	1.0	1.0	1.0	1.0	1.0	1.0	1.0	1.0	1.0	1.0
	Conn.D	$9.0 \cdot 10^{1}$		$1.2 \cdot 10^{2}$		$1.9 \cdot 10^{2}$		$3.8 \cdot 10^{1}$		$4.0 \cdot 10^{1}$	
	SMI	$2.9 \cdot 10^{1}$		$1.8 \cdot 10^{1}$		$5.9 \cdot 10^{1}$		$2.8 \cdot 10^{1}$		5.4	3.0
	Tb.N	$2.2 \cdot 10^{2}$		$4.2 \cdot 10^{2}$		$9.2 \cdot 10^{2}$				$1.2 \cdot 10^{2}$	
	Tb.Th	$6.9 \cdot 10^{2}$		$3.3 \cdot 10^{2}$		$1.0 \cdot 10^{2}$		$6.0 \cdot 10^{2}$		$4.4 \cdot 10^{1}$	
	Tb.Sp	$1.8 \cdot 10^{2}$		$5.0 \cdot 10^{2}$		$8.2 \cdot 10^{2}$		$9.8 \cdot 10^{1}$		$1.2 \cdot 10^{1}$	
	BS	$1.2 \cdot 10^{3}$		$9.9 \cdot 10^{2}$		$1.5 \cdot 10^{3}$		$4.4 \cdot 10^{2}$		$1.7 \cdot 10^{1}$	
	Tb.Th.SD	$3.3 \cdot 10^{1}$		$4.6 \cdot 10^{1}$	2.9	$2.1 \cdot 10^{1}$	1.7	$6.1 \cdot 10^{1}$	2.7	9.0	1.8
	Tb.Sp.SD	$1.2 \cdot 10^{1}$	1.9	$3.2 \cdot 10^{1}$	2.5	$1.3 \cdot 10^{1}$	2.1	$1.9 \cdot 10^{1}$	1.8	$9.3 \cdot 10^{6}$	2.0
ITS	**pBV/TV**	$6.2 \cdot 10^{7}$		$8.3 \cdot 10^{6}$		$9.5 \cdot 10^{6}$		$5.2 \cdot 10^{7}$		$8.3 \cdot 10^{6}$	
	rBV/TV	$7.3 \cdot 10^{6}$		$4.4 \cdot 10^{6}$		$1.2 \cdot 10^{6}$		$3.5 \cdot 10^{7}$		$2.6 \cdot 10^{6}$	
	aBV/TV	$1.7 \cdot 10^{1}$		$1.7 \cdot 10^{2}$		$2.1 \cdot 10^{1}$		$1.9 \cdot 10^{1}$		$1.6 \cdot 10^{1}$	
	pBV/BV	$1.5 \cdot 10^{6}$		$4.3 \cdot 10^{5}$		$9.1 \cdot 10^{4}$		$1.4 \cdot 10^{6}$		$2.3 \cdot 10^{5}$	
	rBV/BV	$1.8 \cdot 10^{7}$		$6.1 \cdot 10^{6}$		$1.8 \cdot 10^{6}$		$4.2 \cdot 10^{7}$		$3.9 \cdot 10^{6}$	
	pTb.N	$6.0 \cdot 10^{6}$		$5.1 \cdot 10^{6}$		$9.5 \cdot 10^{6}$		$4.7 \cdot 10^{6}$		$1.5 \cdot 10^{6}$	
	rTb.N	$3.2 \cdot 10^{3}$		$9.9 \cdot 10^{3}$		$3.3 \cdot 10^{3}$		$1.4 \cdot 10^{3}$		$2.9 \cdot 10^{3}$	
	pTb.Th	$2.8 \cdot 10^{5}$		$2.5 \cdot 10^{5}$	1.7	$3.4 \cdot 10^{5}$		$1.4 \cdot 10^{6}$		$1.2 \cdot 10^{5}$	
	rTb.Th	$1.9 \cdot 10^{2}$	1.4	$2.2 \cdot 10^{3}$		$5.4 \cdot 10^{2}$	2.6	$2.95 \cdot 10^{2}$	3.1	$6.5 \cdot 10^{2}$	
	pTb.S	$5.6 \cdot 10^{5}$		$1.1 \cdot 10^{6}$		$6.0 \cdot 10^{5}$	1.4	$1.6 \cdot 10^{6}$	2.2	$2.4 \cdot 10^{5}$	
	rTb-l	$1.3 \cdot 10^{2}$		$1.8 \cdot 10^{2}$	2.5	$1.5 \cdot 10^{2}$		$5.4 \cdot 10^{1}$	3.0	$1.6 \cdot 10^{2}$	3.6
	RR.Junc.D	$2.5 \cdot 10^{1}$	1.7	$3.1 \cdot 10^{1}$	2.0	$3.1 \cdot 10^{1}$		$5.4 \cdot 10^{1}$		$2.7 \cdot 10^{1}$	2.2
	RP.Junc.D	$6.0 \cdot 10^{2}$		$7.1 \cdot 10^{2}$		$4.4 \cdot 10^{2}$		$3.3 \cdot 10^{2}$		$3.6 \cdot 10^{2}$	
	PP.Junc.D	$1.2 \cdot 10^{3}$		$8.8 \cdot 10^{2}$		$9.8 \cdot 10^{2}$		$3.5 \cdot 10^{2}$		$5.8 \cdot 10^{2}$	
TBS	**TBS_x**	1.8	1.4	2.4	1.8	1.6	1.2	2.7	2	1.6	1.2
	TBS_y	3.0	1.9	3.7	2.1	2.0	1.6	8.6	2.4	3.1	2.3
	TBS_z	2.5	1.5	2.0	1.4	2.2	1.3	5.2	2.2	2.9	1.5

Table 4. Each model was assessed at every anatomical location using adjusted coefficient of determination (r^2_{adj}) and residual standard errors (RSE [MPa]).

		Femur	*Radius*	*Vertebra*	*Iliac crest*	*Combined*
Isotropic	r^2_{adj}	0.914	0.730	0.867	0.917	0.889
	RSE	0.360	0.432	0.362	0.196	0.369
Anisotropic	r^2_{adj}	0.983	0.965	0.955	0.974	0.968
	RSE	0.161	0.155	0.209	0.110	0.199
Global	r^2_{adj}	0.983	0.967	0.957	0.974	0.975
	RSE	0.160	0.151	0.209	0.109	0.195

Supplemental Data

Table A1. Coefficients of determination (r^2) between morphological parameters for the combined dataset. Correlations larger than 0.3 are highlighted and two significance levels are represented by * ($p < 0.05$) and ** ($p < 0.001$).

	DA	*Conn.D*	*SMI*	*Tb.N*	*Tb.Th*	*Tb.Sp*	*BS*	*Tb.Th.SD*	*Tb.Sp.SD*	*pBV/TV*	*rBV/TV*	*aBV/TV*	*pBV/BV*	*rBV/BV*	*pTb.N*	*rTb.N*	*pTb.Th*	*rTb.Th*	*pTb.S*	*rTb.l*	*RRJunc.D*	*RPJunc.D*	*PPJunc.D*	*TBSx*	*TBSy*	*TBSz*
BV/TV	<0.001	0.067**	0.51**	0.512**	0.561**	0.498**	0.439**	0.126**	0.233**	0.99**	0.288**	0.814**	0.341**	0.341**	0.534**	0.113**	0.431**	0.023**	0.109**	0.032**	0.017**	0.259**	0.394**	<0.001	0.17**	0.145**
DA		0.148**	0.007*	0.029**	0.028**	0.008*	0.002	0.026**	0.001	0.001	0.028**	0.006*	0.018**	0.018**	0.069**	0.138**	0.08**	0.071**	0.277**	0.047**	0.098**	0.092**	0.092**	0.002	<0.001	0.028**
Conn.D			0.094**	0.499**	0.079**	0.37**	0.404**	0.123**	0.117**	0.055**	0.118**	0.074**	0.038**	0.038**	0.617**	0.634**	0.169**	0.353**	0.274**	0.451**	0.482**	0.746**	0.763**	0.059**	0.165**	0.028**
SMI				0.405**	0.114**	0.261**	0.7**	<0.001	0.047**	0.536**	0.039**	0.375**	0.393**	0.393**	0.402**	0.068**	0.121**	0.037**	0.054**	0.098**	0.013*	0.236**	0.338**	0.027**	0.031**	0.012*
Tb.N					0.044**	0.804**	0.805**	0.01*	0.439**	0.467**	0.412**	0.57**	0.142**	0.142**	0.821**	0.59**	0.012*	0.061**	0.052**	0.317**	0.185**	0.712**	0.801**	0.035**	0.008*	0.038**
Tb.Th						0.066**	0.021**	0.66**	0.043**	0.555**	0.167**	0.418**	0.122**	0.122**	0.043**	0.004*	0.807**	0.264**	0.323**	0.081**	0.162**	0.001	0.01*	0.018**	0.362**	0.243**
Tb.Sp							0.643**	0.003	0.701**	0.458**	0.356**	0.515**	0.13**	0.13**	0.678**	0.387**	0.054**	<0.001	0.009*	0.17**	0.106**	0.436**	0.538**	0.01*	0.005	0.089**
BS								0.029**	0.247**	0.429**	0.151**	0.423**	0.254**	0.254**	0.675**	0.312**	0.031**	0.053**	0.004	0.264**	0.062**	0.498**	0.615**	<0.001	<0.001	0.023**
Tb.Th.SD									<0.001	0.127**	0.025**	0.072**	0.039**	0.039**	0.002	0.034**	0.373**	0.135**	0.207**	0.103**	0.121**	0.021**	0.014*	0.02**	0.189**	0.084**
Tb.Sp.SD										0.209**	0.206**	0.239**	0.044**	0.044**	0.275**	0.141**	0.046**	0.026**	0.001	0.048**	0.038**	0.125**	0.171**	<0.001	0.019**	0.076**
pBV/TV											0.202**	0.789**	0.414**	0.414**	0.52**	0.073**	0.428**	0.019**	0.143**	0.035**	0.039**	0.216**	0.361**	0.002	0.184**	0.132**
rBV/TV												0.318**	0.048**	0.048**	0.197**	0.531**	0.118**	0.032**	0.065**	<0.001	0.235**	0.39**	0.284**	0.067**	0.005	0.118**
aBV/TV													0.254**	0.254**	0.495**	0.144**	0.36**	0.03**	0.049**	0.057**	0.001	0.272**	0.382**	0.017**	0.049**	0.295**
pBV/BV														1**	0.353**	0.008*	0.085**	0.009*	0.229**	0.223**	0.144**	0.046**	0.157**	0.047**	0.056**	0.018**
rBV/BV															0.353**	0.008*	0.085**	0.009*	0.229**	0.223**	0.144**	0.046**	0.157**	0.047**	0.056**	0.018**
pTb.N																0.495**	0.004	0.128**	0.033**	0.492**	0.11**	0.733**	0.892**	0.009*	0.002	0.01*
rTb.N																	0.04**	0.22**	0.433**	0.304**	0.674**	0.851**	0.694**	0.073**	0.137**	<0.001
pTb.Th																		0.497**	0.41**	0.122**	0.218**	0.013*	0.003	0.03**	0.396**	0.373**
rTb.Th																			0.306**	0.374**	0.236**	0.252**	0.227**	0.004	0.328**	0.297**
pTb.S																				0.161**	0.552**	0.205**	0.113**	0.053**	0.296**	0.109**
rTb.l																					0.21**	0.408**	0.451**	0.003	0.17**	0.021**
RRJunc.D																						0.414**	0.254**	0.109**	0.341**	0.019**
RPJunc.D																							0.934**	0.052**	0.086**	<0.001
PPJunc.D																								0.036**	0.039**	0.001
TBSx																									0.032**	0.006*
TBSy																										0.046**